

# Neutron Diffraction Reveals Hydrogen Bonds Critical for cGMP-Selective Activation: Insights for cGMP-Dependent Protein Kinase Agonist Design

Gilbert Y. Huang,<sup>#,†</sup> Oksana O. Gerlits,<sup>#,‡</sup> Matthew P. Blakeley,<sup>§</sup> Banumathi Sankaran,<sup>||</sup> Andrey Y. Kovalevsky,<sup>‡</sup> and Choel Kim<sup>\*,†,⊥</sup>

<sup>†</sup>Verna and Mars McClean Department of Biochemistry and Molecular Biology, Baylor College of Medicine, One Baylor Plaza, Houston, Texas 77004, United States

<sup>‡</sup>Biology and Soft Matter Division, Oak Ridge National Laboratory, Oak Ridge, Tennessee 37831, United States

<sup>§</sup>Institute Laue-Langevin, 71 Avenue des Martyrs, 38000, Grenoble, France

<sup>||</sup>Berkeley Center for Structural Biology, Lawrence Berkeley National Laboratory, Berkeley, California, United States

<sup>⊥</sup>Department of Pharmacology, Baylor College of Medicine, One Baylor Plaza, Houston, Texas 77004, United States

## Supporting Information

**ABSTRACT:** High selectivity of cyclic-nucleotide binding (CNB) domains for cAMP and cGMP are required for segregating signaling pathways; however, the mechanism of selectivity remains unclear. To investigate the mechanism of high selectivity in cGMP-dependent protein kinase (PKG), we determined a room-temperature joint X-ray/neutron (XN) structure of PKG I $\beta$  CNB-B, a domain 200-fold selective for cGMP over cAMP, bound to cGMP (2.2 Å), and a low-temperature X-ray structure of CNB-B with cAMP (1.3 Å). The XN structure directly describes the hydrogen bonding interactions that modulate high selectivity for cGMP, while the structure with cAMP reveals that all these contacts are disrupted, explaining its low affinity for cAMP.

In mammals, the cAMP- and cGMP-dependent protein kinases (PKA and PKG) are major mediators of cyclic nucleotide signaling critical for physiological processes such as memory formation and vasodilation.<sup>1</sup> Clinically, aberrant PKA signaling causes Carney complex, while mutations in PKG cause thoracic aortic aneurysms and dissections (TAAD).<sup>2–4</sup> PKA is better understood than PKG—structures of PKA in the cAMP bound and holoenzyme forms showed how, without cAMP, the cyclic-nucleotide binding (CNB) domains in the regulatory (R) subunit of PKA bind and inhibit the catalytic (C) subunit, and subsequently, how cAMP binding drives conformational change in the R subunit to release the C subunit, allowing phosphorylation.<sup>5–7</sup>

In contrast, only PKG structures of truncated CNB domains are available.<sup>8–10</sup> Unlike in PKA, the R- and C-domains in PKG are fused into one polypeptide. Low-resolution structural data have shown that PKG undergoes large conformational changes upon cGMP binding to its tandem CNB domains (CNB-A/B), driving kinase activation.<sup>11</sup> In agreement, recent structures show that the C-terminal CNB domain of PKG I (CNB-B) undergoes large rearrangement upon cGMP binding, providing a glimpse into the structural changes required for kinase

activation.<sup>10</sup> Furthermore, while CNB-A binds both cGMP and cAMP comparably, the C-terminal CNB-B domain is 200-fold selective for cGMP over cAMP. However, the mechanism of reduced affinity for cAMP remains unknown. Because hydrogen bonds with the guanine moiety enhance affinity for cGMP in other CNB domains, we directly studied the hydrogen bonding interactions between PKG and cGMP.<sup>12,13</sup> Here we present a room-temperature joint X-ray/neutron (XN) structure of CNB-B in complex with cGMP (PDB: 4QXK) at 2.2 Å resolution, the first neutron structure of any CNB domain, and a low-temperature X-ray structure of CNB-B with cAMP at 1.3 Å resolution (Figures 1 and S1, PDB: 4QXS). The XN structure with cGMP provides direct determination of deuterium positions and visualization of all hydrogen bonds. Comparison of the XN structure with the low-temperature X-ray structures reveals that the interaction of Arg297 with cGMP is more dynamic than previously appreciated, while Arg297 interacts with cAMP only through van der Waals (VDW) interactions. Furthermore, cAMP binds as both *syn* and *anti* conformers, further weakening the interaction with CNB-B. Taken together, these structures provide new mechanistic insight into the ability of CNB-B to filter out cAMP. Because PKG activation causes vasodilation in vascular smooth muscle cells, these structures will assist the rational design of PKG activators in the treatment of hypertensive disease.

The recent low-temperature X-ray structure of CNB-B in complex with cGMP indicated interactions with the binding pocket potentially crucial for cGMP selectivity.<sup>10</sup> To directly visualize hydrogen bonds in CNB-B, we solved the XN structure of CNB-B:cGMP (Figures 1 and S1). The sugar-phosphate moiety of cGMP is captured by residues of the phosphate binding cassette (PBC) motif, comprising residues 306–317 (Figure S2A and Table S2). In the PBC, a hydrogen bond is formed between the main-chain amide of Gly306 and the 2'-hydroxyl group of D-ribose, with an N…O distance of 2.9

**Received:** August 15, 2014

**Revised:** September 26, 2014

**Published:** October 1, 2014



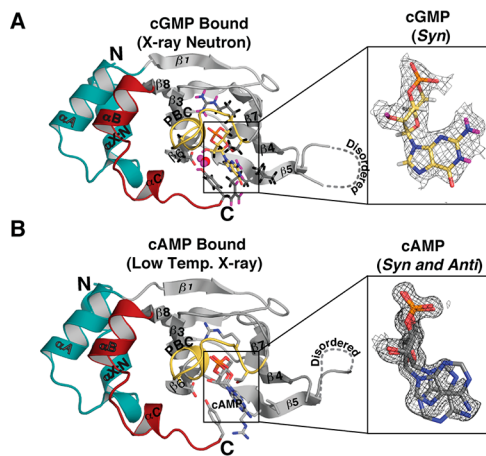


**Figure 1.** PKG I $\beta$  (219–369):cGMP and PKG I $\beta$  (219–369):cAMP complexes. (A) XN structure of PKG I $\beta$  (219–369):cGMP at room temperature (293 K), with interacting side chains rendered in sticks and colored by atom type, with carbon gray, oxygen red, nitrogen blue, hydrogen black, and deuterium magenta. The  $2|F_0| - |F_1|$  nuclear density for cGMP (syn) is contoured at  $1\sigma$  and shown as a gray mesh. (B) X-ray structure PKG I $\beta$  (219–369):cAMP at low temperature (100 K). The  $2|F_0| - |F_1|$  electron density map for cAMP (anti and syn) is contoured at  $1\sigma$  and shown as a gray mesh.

Å. Furthermore, the 2'-hydroxyl donates deuterium in a relatively short hydrogen bond with the carboxylate side chain of Glu307 (O···O separation of 2.4 Å), which is oriented by a similarly short hydrogen bond with the phenolic oxygen of Tyr351 and a 2.8 Å hydrogen bond with its own main-chain amide (Figures 2A and S3). At the top of PBC, the phosphate oxygen atoms in cGMP each form two hydrogen bonds. The equatorial oxygen forms hydrogen bonds with the main-chain

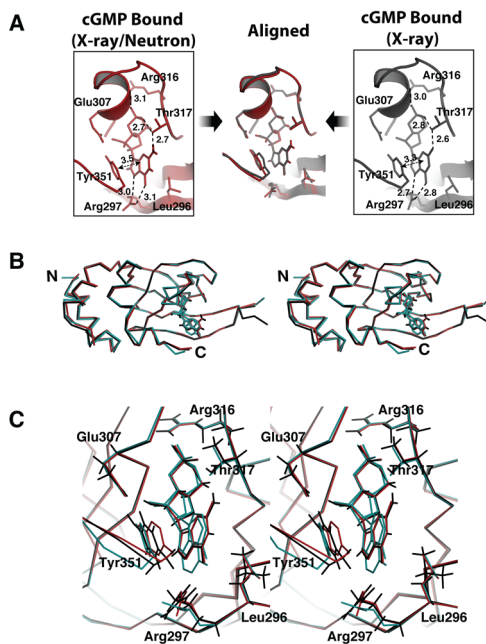


**Figure 2.** XN versus low temperature X-ray structures. (A) Room temperature XN (left, PDB: 4QXK) and low-temperature X-ray structures (right, PDB: 4KU7) bound to cGMP. (B) Superposition of the XN (black) and low temperature structures (red-cGMP bound, cyan-cAMP bound) in stereo. (C) Zoomed in view of cGMP pocket and interacting residues in stereo.

amide of Ala309 and the guanidinium moiety of Arg316, while the axial oxygen hydrogen bonds to the main-chain amide and the side-chain hydroxyl of Thr317. All four hydrogen bonds are similar in length in the XN structure, ranging from 2.8 to 3.0 Å, although the bonds formed by Thr317 are shorter in the low-temperature X-ray structure, with distances of 2.6–2.8 Å (Figures S2A and 2A). In addition to donating its deuterium in a hydrogen bond with cGMP, the hydroxyl of Thr317 accepts a deuterium in a hydrogen bond with guanine's 2-ND<sub>2</sub> group of cGMP bridging the cyclic phosphate and guanine moieties (Figure S4). Consistent with this, it was demonstrated that Thr317 and the analogous residue at the N-terminal CNB-A, Thr193, are key residues responsible for high affinity for cGMP.<sup>14</sup> Thus, hydrogen bonding between Thr317 and cGMP is very important for cGMP affinity to CNB-B.

Another key interaction with the guanine moiety of cGMP occurs at the flexible side chain of Arg297 (Figures 2A and S2A). The low-temperature X-ray structure showed short hydrogen bonds between the Arg297's guanidinium group and O6 and N7 of guanine at distances of 2.7–2.8 Å, indicating tight hydrogen bonding interactions. At room temperature, however, Arg297's side-chain moves slightly outward, showing increased distances of 3.0–3.1 Å, implying that interactions between Arg297 and guanine are weaker than the low-temperature X-ray structure suggested (Figures 2A and Table S2). Therefore, we propose the Arg297's side-chain position is a "frozen out" conformation in the low-temperature structure. Indeed, this is consistent with structures solved at low temperature.<sup>15</sup> The cGMP binding is further stabilized by Tyr351 at the  $\alpha$ C helix (Figure S2A). Tyr351's phenol group makes  $\pi$ – $\pi$  interactions with the guanine moiety, sandwiching the nucleotide against Val283 and Leu296 on strands  $\beta$ 4 and  $\beta$ 5. Furthermore, the phenol group is stabilized through hydrogen bonds with an ordered water molecule and Glu307 in the binding pocket. Our XN structure shows that the amide hydrogens of the peptide backbone behind cGMP at residues 305–310 are not exchanged with deuterium, suggesting the cGMP pocket is not accessible to solvent, agreeing with earlier H/D exchange mass spectrometry studies on the full-length regulatory domain of PKG I $\beta$ .<sup>16</sup> Thus, the protein dynamics are slowed substantially in the pocket when cGMP is bound, and tight interaction with cGMP shields the pocket from solvent.

To further investigate the cGMP selectivity mechanism of CNB-B, we solved a low-temperature X-ray structure bound with cAMP at 1.3 Å (Figures 1B and S2B). The main differences from the XN structure occur at the contacts with the purine base moieties (Figure S2B). In the cGMP complex, hydrogen bonding between the 2-NH<sub>2</sub> group of guanine and Thr317 ensures that cGMP is bound in the syn-conformation; however, cAMP lacks this NH<sub>2</sub> group and binds to the pocket in both syn- and anti-conformations (Figure 1). Consequently, the adenine moiety in the syn-conformation forms a weaker C–H···O hydrogen bond with Thr317 (3.3 Å) (Figure S2B and Table S2). Likewise, the anti-conformer also makes a weak contact using its C8–H methine group (3.6 Å). Notably, Arg297 moves away from adenine to avoid collision and is positioned only within VDW distance of cAMP (Figure S2B and 2B). Finally, while the capping interaction of Tyr351 with cAMP still forms similar to the cGMP-bound structure, superimposing the two structures reveals that Tyr351 is positioned slightly further from the binding pocket in the presence of cAMP (Figure 2B,C). Thus, cAMP, like cGMP, rotates Arg297 outward and recruits Tyr351, though the

weakened contacts with Arg297, Thr317, and Tyr351 suggest that the cAMP-bound conformation is energetically less stable than the cGMP-bound conformation.

Our new data provide additional details for the high selectivity mechanism for cGMP.<sup>8,10</sup> From these structures, we conclude that cGMP stabilizes the flexible side chain of Arg297 through hydrogen bonds, while cAMP forms VDW contacts with Arg297, creating a higher energy state than cGMP. Thus, our new structures clarify the mechanism of how CNB-B filters out cAMP. Additionally, hydrogen bonds formed by exocyclic oxygens of the cyclic phosphate moiety combined with the observed conformational changes in the PBC associated with cGMP binding may explain previous observations that (Rp)-cGMPS or (Sp)-cGMPS analogues of cGMP act as either agonists or antagonists of PKG I.<sup>10,17</sup> For example, (Rp)-cGMPS, which has the equatorial exocyclic oxygen of cGMP replaced with sulfur, is a competitive inhibitor with a  $K_i$  value of 20  $\mu\text{M}$  while (Sp)-cGMPS, which has the axial exocyclic oxygen of cGMP replaced with sulfur, is a weak agonist with over 100-fold less potency than cGMP.<sup>17</sup> Since sulfur-mediated hydrogen bonds are weaker than oxygen-mediated hydrogen bonds, we speculate that in the case of the (Rp)-cGMPS, replacing the equatorial exocyclic oxygen with sulfur would disrupt the hydrogen bonding interaction with Ala309, which may be crucial for causing the conformational change at the PBC that leads to activation (Figure S5).<sup>18</sup> Thus, the weakened interaction with Ala309 may allow (Rp)-cGMPS to be an antagonist. Additionally, in the case of (Sp)-cGMPS, replacing the equatorial oxygen with sulfur would weaken its interaction with Arg316 and Thr317 without affecting its interaction with Ala309. Thus, unlike (Rp)-cGMPS, (Sp)-cGMPS weakly activates PKG.

To conclude, our CNB-B:cGMP neutron structure, the first neutron structure of a CNB domain, provides an unprecedented view of the hydrogen bonding interactions that could serve as a model for other CNB domains, accomplished through direct observation of hydrogen bonds that mediate cyclic nucleotide coordination. Furthermore, because of the importance of PKG as a drug target,<sup>19</sup> the directly observed hydrogen bonds provide new information required for the rational design of PKG activators. Small molecules will need to accommodate these interactions to activate PKG—consistent with this idea, cAMP does not stabilize the same interactions as cGMP and can only weakly activate PKG. Thus, the new insight into the structure and dynamics of PKG is vital for rational design of PKG activators and for explaining the differences in kinase activation.

## ■ ASSOCIATED CONTENT

### Supporting Information

Methods for all experiments and supporting figures and tables (Figures S1–S8, Tables S1 and S2) are available free of charge via the Internet at <http://pubs.acs.org>.

## ■ AUTHOR INFORMATION

### Corresponding Author

\*E-mail: ckim@bcm.edu. Phone: 713-798-8411.

### Author Contributions

#G.Y.H. and O.O.G. contributed equally.

### Funding

This work was supported by NIH Grants R01GM090161 (to C.K.) and T32GM008280 (to G.Y.H.). O.O.G. and A.Y.K. are

supported by the DOE Office of Basic Sciences. The Advanced Light Source is supported by DOE Contract No. DE-AC02-05CH11231, the NIGMS, and the HHMI.

### Notes

The authors declare no competing financial interest.

## ■ ABBREVIATIONS

CNB, cyclic-nucleotide binding; cAMP, cyclic adenosine monophosphate; cGMP, cyclic guanosine monophosphate; VDW, van der Waals; PKG, cGMP-dependent protein kinase; PKA, cAMP-dependent protein kinase; CAP, catabolite activator protein; XN, joint X-ray/neutron; PBC, Phosphate Binding Cassette

## ■ REFERENCES

- (1) Beavo, J. A., and Brunton, L. L. (2002) *Nat. Rev. Mol. Cell Biol.* 3, 710–718.
- (2) Kirschner, L. S., Carney, J. A., Pack, S. D., Taymans, S. E., Giatzakis, C., Cho, Y. S., Cho-Chung, Y. S., and Stratakis, C. A. (2000) *Nat. Genet.* 26, 89–92.
- (3) Casey, M., Vaughan, C. J., He, J., Hatcher, C. J., Winter, J. M., Weremowicz, S., Montgomery, K., Kucherlapati, R., Morton, C. C., and Basson, C. T. (2000) *J. Clin. Invest.* 106, R31–38.
- (4) Guo, D. C., Regalado, E., Casteel, D. E., Santos-Cortez, R. L., Gong, L., Kim, J. J., Dyack, S., Horne, S. G., Chang, G., Jondeau, G., Boileau, C., Coselli, J. S., Li, Z., Leal, S. M., Shendure, J., Rieder, M. J., Bamshad, M. J., Nickerson, D. A., GenTAC Registry Consortium, National Heart, Lung, and Blood Institute Grand Opportunity Exome Sequencing Project, Kim, C., and Milewicz, D. M. (2013) *Am. J. Hum. Genet.* 93, 398–404.
- (5) Su, Y., Dostmann, W. R., Herberg, F. W., Durick, K., Xuong, N. H., Ten Eyck, L., Taylor, S. S., and Varughese, K. I. (1995) *Science* 269, 807–813.
- (6) Kim, C., Xuong, N. H., and Taylor, S. S. (2005) *Science* 307, 690–696.
- (7) Kim, C., Cheng, C. Y., Saldanha, S. A., and Taylor, S. S. (2007) *Cell* 130, 1032–1043.
- (8) Kim, J. J., Casteel, D. E., Huang, G., Kwon, T. H., Ren, R. K., Zwart, P., Headd, J. J., Brown, N. G., Chow, D. C., Palzkill, T., and Kim, C. (2011) *PLoS One* 6, e18413.
- (9) Osborne, B. W., Wu, J., McFarland, C. J., Nickl, C. K., Sankaran, B., Casteel, D. E., Woods, V. L., Jr., Kornev, A. P., Taylor, S. S., and Dostmann, W. R. (2011) *Structure* 19, 1317–1327.
- (10) Huang, G. Y., Kim, J. J., Reger, A. S., Lorenz, R., Moon, E. W., Zhao, C., Casteel, D. E., Bertinetti, D., Vanschouwen, B., Selvaratnam, R., Pflugrath, J. W., Sankaran, B., Melacini, G., Herberg, F. W., and Kim, C. (2014) *Structure* 22, 116–124.
- (11) Alverdi, V., Mazon, H., Versluis, C., Hemrika, W., Esposito, G., van den Heuvel, R., Scholten, A., and Heck, A. J. (2008) *J. Mol. Biol.* 375, 1380–1393.
- (12) Flynn, G. E., Black, K. D., Islas, L. D., Sankaran, B., and Zagotta, W. N. (2007) *Structure* 15, 671–682.
- (13) Pessoa, J., Fonseca, F., Furini, S., and Morais-Cabral, J. H. (2014) *J. Gen. Physiol.* 144, 41–54.
- (14) Reed, R. B., Sandberg, M., Jahnsen, T., Lohmann, S. M., Francis, S. H., and Corbin, J. D. (1996) *J. Biol. Chem.* 271, 17570–17575.
- (15) Fraser, J. S., van den Bedem, H., Samelson, A. J., Lang, P. T., Holton, J. M., Echols, N., and Alber, T. (2011) *Proc. Natl. Acad. Sci. U. S. A.* 108, 16247–16252.
- (16) Lee, J. H., Li, S., Liu, T., Hsu, S., Kim, C., Woods, V. L., and Casteel, D. E. (2011) *Int. J. Mass Spectrom.* 302, 44–52.
- (17) Butt, E., van Bemmelen, M., Fischer, L., Walter, U., and Jastorff, B. (1990) *FEBS Lett.* 263, 47–50.
- (18) Allen, F., Bird, C., Rowland, R., and Raithby, P. (1997) *Acta Crystallogr., Sect. B* 53, 680–695.
- (19) Schlossmann, J., and Hofmann, F. (2005) *Drug Discovery Today* 10, 627–634.